Novel in situ tribo-catalysis for improved tribological properties of bio-oil model compound

Peng, Yubin; Xu, Yufu; Dearn, Karl; Geng, Jian; Hu, Xianguo

DOI:
10.1016/j.fuel.2017.10.080

Document Version
Peer reviewed version

Citation for published version (Harvard):
Peng, Y, Xu, Y, Dearn, KD, Geng, J & Hu, X 2018, 'Novel in situ tribo-catalysis for improved tribological properties of bio-oil model compound', Fuel, vol. 212, pp. 546-553. https://doi.org/10.1016/j.fuel.2017.10.080

Novel in situ tribo-catalysis for improved tribological properties of bio-oil model compound

Yubin Peng[a], Yufu Xu[a,*], Karl D Dearn[b], Jian Geng[a], Xianguo Hu[a]

a. Institute of Tribology, School of Mechanical Engineering, Hefei University of Technology, Hefei 230009, China

b. Mason Institute of Tribology, Mechanical Engineering, School of Engineering, University of Birmingham, Edgbaston, Birmingham, B152TT, United Kingdom

Abstract: A novel in-situ tribocatalytic esterification reaction has been developed driven by frictional processes, to alleviate the corrosion wear induced by the high content of organic acid in bio-oil. Solid superacid (SO_4^{2-}/γ-Al_2O_3) was formulated and prepared as the catalyst. Acetic acid was as the base for the bio-oil, and glycerol was used as a modifying agent. The tribological properties of the bio-oil with varying amounts of solid superacid were evaluated on a HDM-20 end-face tribometer. SEM (Scanning electron microscope) and XPS (X-ray photoelectron spectroscopy) were used to measure the micro-morphologies and elemental contents on the worn surfaces after sliding. The effect of tribocatalysis on the composition of the bio-oil was analyzed by FTIR (Fourier Transform Infrared Spectrometer) and GC-MS (Gas Chromatography-Mass Spectrometry). The results show that when lubricated by pure bio-oil the worn surfaces showed severe furrows and bulk exfoliation. With the solid superacid added to the bio-oil, abrasive wear and exfoliation were alleviated. From a tribological perspective, the optimum blend volume was 1wt% solid superacid. The reason for the improved tribological properties solid superacid not only could roll on the friction surface and act as lubricating particles, but also catalyzed esterification

* Corresponding author. Tel.: +86 551 62901359; fax: +86 551 62901359.
E-mail: xuyufu@hfut.edu.cn

between acetic acid and glycerol, which simultaneously improved the tribological properties of bio-oil.

Keywords: Bio-oil; solid superacid; Esterification; Tribocatalysis

1. Introduction

Bio-oil is a promising alternative to fossil fuels processing a range of renewable and environmentally-friendly advantages. Fast pyrolysis technology is a general way to produce bio-oil from biomass [1]. Pyrolysis technology is a simple, convenient and very effective method, the production of bio-oil from pyrolysis is very complicated. When produced, the bio-oil is mainly composed of organic acids, alcohols, phenols, alkanes, aldehydes and ketones [2, 3]. In this form, crude bio-oil, can not be directly deployed as a fuel for internal combustion engines (replacing for example diesel oil) because of its undesirable characteristics, such as high corrosion, high viscosity and low heating value [4]. If it were to be used as a crude fuel the engine would likely suffer from, amongst other things, severe corrosive wear of the friction pairs in the engine such as the piston rings and cylinder liners, leading to a decrease in the service life of the engines [5]. Upgrading and enhancing the quality of crude bio-oil is a vital step towards a wider adoption of this promising biofuel.

Catalytic esterification has been shown to be an effective process for improving the properties of bio-oil, by converting organic acids into the corresponding esters [4, 6]. Song et al. [7] used esterification to upgrade bio-oil with a SO_4^{2-}/SiO_2-TiO_2 catalyst. In doing so the pH value of the subsequent bio-oil increased from 3.22 to 5.43, and demonstrated enhanced stability. Wang et al. [8] where able to decrease the

acid numbers of upgraded bio-oil by 88.54% and 85.95% with 732 and NKC-9 type ion exchanger resins, respectively. The choice of catalyst used in the esterification process can be vitally important. From a tribological perspective, Xu et al. [9] compared the tribological properties of crude and esterified bio-oil. Results showed that esterified bio-oil had better friction-reducing and anti-wear properties compared to the crude oil. The tribological improvement was as result of the decrease in acidic corrosion combined with the formation of a protective tribo-film that included ester and other organic groups. Bio-oil could therefore be used in IC engines with the correct upgrade using optimized catalytic esterification.

Tribocatalysis is an emerging aspect of tribochemistry, linking the properties of a catalyst to the effects of rubbing energy [10]. Onodera et al. [11] investigated the tribocatalytic activity of γ-Al_2O_3 and α-Al_2O_3 for the degradation of PTFE. It was found that γ-Al_2O_3 had a stronger catalytic activity at lower temperatures during friction. This resulted in a discontinuous transfer film and inferior tribological properties. Hiratsuka et al. [12] studied catalytic oxidation of ethylene, with palladium sliding against Al_2O_3. The catalytic effect was strengthened, and the products of catalytic reaction were more completely oxidized as a result of rubbing. In essense, mechanical energy in the complicated friction system enhanced the activity of the catalyst.

These tribocatalytic princples could be applied to the esterification process to promote catalyst activity leading to improved tribological properties. However, to the best of our knowledge, few reports have described the tribocatalytic esterification of

bio-oil for improved fuel design. In this paper, solid superacid (SO_4^{2-}/γ-Al_2O_3) was prepared as the catalyst and the effect of tribocatalytic esterification on bio-oil was studied during friction process. Optimum catalytic concentrations for tribological properties of bio-oil have also been studied.

2. Experimental

2.1. Materials

The γ-Al_2O_3 powders with an average particle size of 10 nm, used for the catalysts were supplied by Shanghai Macklin Biochemical Co., Ltd. The chemical agents including sulphuric acid, acetic acid and glycerol were purchased from Sinopharm Chemical Reagent Co., Ltd. All reagents were analytical grade.

For the tribological testing, the lower samples were machined 36 mm diameter, 3 mm thick discs made using QT600 nodular cast iron. The upper specimens were ASTM 1045 medium carbon steel, which was quenched to give a hardness of 47-53HRC, machined to the geometry shown in **Fig. 1**.

2.2. Catalyst preparation

The solid superacid SO_4^{2-}/γ-Al_2O_3 was prepared using the impregnation method defined fully in [13]. γ-Al_2O_3 powders (1g) were dispersed in a diluted H_2SO_4 solution (20mL, 3mol/L). The mixture was further stirred for 3 h to ensure full contact between the particles and acid solution. After aging overnight, the treated powders were centrifuged out, and then dried at 110°C for 12h and was then ground in an agate

grinding bowl. The solid superacid was finally synthesized after calcination at 500°C for 5 h.

2.3. Tribological tests

To simplify the formulation of and the interpretation of the performance of the tribocatalytic esterification of bio-oil (comprising of many kinds of organic components), acetic acid was selected as a model bio-oil, and glycerol was used as a modifying agent. The lubricating medium during the frictional tests was configured by with mass ratio of 1:1 acetic acid and glycerol. Hence forth, in this paper this formulation will be referred to as bio-oil for convenience. The solid superacid catalyst was ultrasonically dispersed in the bio-oil for 10 min with different mass fractions (0wt%, 0.5wt%, 1wt%, 1.5wt%, 2wt%) at room temperature. The friction and wear properties were tested on a HDM-20 end tribometer. **Fig.1** shows the schematic diagram of the tribometer and the friction pairs. The lower specimen was fixed in the oil box. Three small bosses (4×4mm) protruding from the upper specimen slid against the lower specimen with a rotational speed of 441rpm during the frictional process. Further details of the test conditions are listed in **Table 1**.

Before the friction tests, the upper specimen prepared by mounting it first on the tribometer and then running the three raised bosses against 500 grit metallographic sandpaper. Doing so ensured a true plane between the frictional surfaces and a consistent surface roughness. After this and before testing, the upper and lower specimens were cleaned with acetone. During the experiments, the friction coefficient

was measured in real-time. The wear loss was calculated by measuring the change in weight of the lower specimens before and after the tribo-tests. Each test was repeated three times to obtain a standard deviation. After the experiments the lower specimens were ultrasonically cleaned with acetone for 30min enable further characterization and analysis. Finally, the bio-oil was collected and then centrifuged at 8000 rpm for 30 min to remove remaining solid superacid and wear debris.

2.4 Characterization of materials and frictional surfaces

The size distribution of the solid superacid was measured using a Zeta potentiometer (Nano-ZS90). The Fourier Transform Infrared Spectrometer (Nicolet 67) was used to characterize the functional groups of the solid superacid. To evaluate catalytic activity, an esterification experiment of bio-oil with 2wt% solid superacid was carried out in a stirred glass reactor for 5h at 120 °C. The conversion rate of acetic acid with time was calculated by:

$$C_i = \frac{M_0 - M_i}{M_0} \times 100\%$$

Where C_i is the conversion rate of acetic acid with time (i); M_0 is the acid value of the original bio-oil before frictional testing; M_i is the acid value of bio-oil with time. The acid value was measured by titration with 0.05 mol/L KOH solution [8].

The micro-topographies of the worn surfaces of the lower specimens was measured using a Scanning electron microscope (JEOL JSM-5600LV). X-ray photoelectron spectroscopy (ESCA-LAB 250 Xi) was employed to analyze the bonding energy of main elements on worn surfaces.

In order to evaluate the catalytic efficiency of the solid superacid, the functional groups from the post-test bio-oil were analyzed using the FTIR Spectrometer. The compositions of the bio-oil after testing were characterized by Gas Chromatography Mass Spectrometry (7890A-5975C). For the GC-MS measurement, a 1μL sample was injected into the column with helium. The flow rate was set as 1mL/min, and the split ratio was 20:1. The column was heated from 40°C to 280°C at a linear rate of 10 °C /min, and the measurement ran for 30min.

3. Results and discussion

3.1. Characterization of catalyst

Fig.2 shows the SEM micro-morphology and EDS spectra of the solid superacid. It can be seen that the size of the solid superacid varied widely, from a few microns down to less than 1 μm. Considering the original size of γ-Al_2O_3 powders, it seemed that the powders tended to agglomerate into the bigger particles after supporting sulfate ions. Sulfur was detected in the EDS spectrum, suggesting that the sulfate ions had been supported on γ- Al_2O_3 particles.

Fig. 3a shows the size distribution of the solid superacid. The average particle size of the solid superacid was 3.091μm with a range from 0.255μm to 6.439μm, which was in accordance with the SEM images in Fig.2. The content of the solid superacid with particle sizes of less than 1 μm was approximately 11.5 vol%.

Fig. 3b shows the FTIR spectra of the solid superacid and γ-Al_2O_3 powders. For the solid superacid, the existence of new characteristic peaks at 1049, 1090, and

1180cm^{-1} belonged to S=O band stretching vibrations, which proved that the sulfate groups have been supported on the γ-Al_2O_3 [13, 14]. The peak at 1634cm^{-1} was ascribed to the bending vibration of hydroxyl group (O-H) from absorbed water. Compared with the γ-Al_2O_3 powders, the stretching vibration peak for the solid superacid's hydroxyl group shift from 3448 to 3415cm^{-1}, may have resulted from the formation of the S-O-H functional group [15].

Fig. 3c shows the conversion rate of acetic acids against time with 2wt% the solid superacid at 120°C. The conversion rate increased quickly during the first half an hour, and kept a stable value of 46% after 1.5h, suggesting good catalytic activity for the solid superacid.

3.2. Friction and wear with different contents of the solid superacid

Fig. 4 shows the average friction coefficients and wear losses for bio-oil with different contents of the solid superacid. As the concentration of solid superacid increased, the average friction coefficient and wear loss decreased. The optimum blend ratio was 1wt% solid superacid for the best tribological properties. Nevertheless, when the content was higher than 1wt%, the average friction coefficient and wear loss increased. The behaviour indicated that SO_4^{2-}/γ-Al_2O_3 could improve the friction-reducing and anti-wear properties of bio-oil at suitable contents (1wt%). The improved effect might be attributed to that the solid superacid being absorbed into the friction interface and forming a protective film, which is similar to the lubricating effects of Al_2O_3 nanoparticles [16]. Despite the γ-Al_2O_3 increasing in size due to

sulfate ions, it will still have played a role in reducing friction and wear.

3.3. Tribological mechanisms

Fig. 5 shows the micro-morphologies of worn surfaces with different contents of the solid superacid catalyst. It can be seen that when lubricated with pure bio-oil, there were some severe furrows and bulk exfoliations on the worn surface, which attributed to acidic corrosion [17]. The acetic acid in bio-oil degraded the frictional surfaces in form of cracking and fracture, which reduced the wear-resisting property and generated a lot of abrasive grains and bulk exfoliations during the frictional process [18]. The severe abrasive wear that resulted from grains and bulk exfoliations made the frictional surfaces rougher and in turn promoted the acid corrosion [19]. The synergistic effect of friction and corrosion led to the poor tribological properties for the bio-oil.

As the solid superacid was blended in to the bio-oil, the morphologies of worn surfaces changed significantly. A form of delamination occurred on the worn surfaces, replacing bulk exfoliations. The severe furrowing observed in the previous test were reduced becoming less dense and slimer as seen in Fig.5 (b, c). This maybe due to a polishing effect when the solid superacid is added [20, 21]. However, once the content of the solid superacid exceeded 1wt%, delamination gradually changed, reverting to bulk exfoliations, and deep, severe furrows as seen in Fig.5 (d, e). This phenomenon was indicative of the variation in the tribological properties for bio-oil with different concentration of the solid superacid as seen in Fig. 4. These observations suggest that the solid superacid may permeate and roll on the frictional

surface, preventing friction pairs from contacting directly and improving the tribological properties of the bio-oil [16, 22]. Tribological properties dropped once the concentration of the solid superacid exceeded 1wt%, most likely as the result of agglomeration of particles, which led to severe abrasive wear as seen in Fig. 4 [23]. Despite this, the addition of solid superacid improved wear-resistance at all concentrations compared with pure bio-oil.

The FTIR spectra of the bio-oil with different concentrations of solid superacid before and after tribo-tests are shown in **Fig. 6(a)**. The peaks at 1714 and 1753 cm^{-1} belonged to carbonyl (C=O) that come from carboxyl group (-COOH) and ester group (-COOC), respectively [14, 24]. It can be seen that all bio-oil spectra had the characteristic peak of ester group after the tribo-tests. This suggests that esterification occured during the frictional process, regardless of the presence of the solid superacid in the bio-oil. Rane et al. [13] have reported that esterification conversion of glycerol could reach 82% without the solid superacid at 110 °C, when the molar ratio of acetic acid and glycerol is 1:9. Similarly, Kuzharov et al [25] found some complicated chemical transformations happening under the frictional system when lubricated by Glycerol. The spontaneous trend of esterification at appropriate conditions and the complicated frictional environment amy be a reason that the ester group was detected in thebio-oil without the solid superacid.

Fig. 6(b) shows gas chromatograms of the bio-oil with different contents of the solid superacid after the tribo-tests. Compared with the standard mass spectrometry, the peak at 10.2 min belonged to glyceryl monoacetate as seen in **Fig. 6(c)**, and the

other peaks around at 3.2 min, 3.8 min and 9.5 min were ascribed to alcohol, acetic acid and glycerol, respectively. The existence of glyceryl monoacetate in all the gas chromatograms corresponded with the FTIR spectra in Fig.6 (a). The alcohol detected in gas chromatograms was the solvent for the measurement. The esterification conversion rate after tribo-test could be evaluated by the integral area ratio of glyceryl monoacetate (I_{gm}) and glycerol (I_g) in gas chromatograms. When 1wt% solid superacid was added in bio-oil, the content of glyceryl monoacetate increased as seen in Fig.6 (b), which indicated that the solid superacid promoted esterification and decreased acid content during the frictional process. The generated ester could be absorbed on the friction surface and if so would lead to improved tribological properties [26]. However, once the content of the solid superacid was at and beyond 2wt%, the content of glyceryl monoacetate decreased, which might be attributed to the inactivity of the solid superacid resulting from the severe abrasive wear as seen in Fig. 3.

Fig. 7 shows the XPS spectra of typical elements on worn surfaces. In the C1s spectra, the peaks at 284.7eV, 285.7eV, 288.3eV and 289.1eV belonged to C-C/C-H, C-O, COOH and COOC groups, respectively [27, 28]. These confirmed that the acid and generated ester could be absorbed onto the frictional surfaces. The relative atomic percentages of carbon with different valence states on the worn surfaces are shown in **Table 2**. When lubricated without the solid superacid, the relative percentage of COOH group was highest, suggesting the most severe acid corrosion of the friction pairs. As the solid superacid was added into the bio-oil, the percentage of COOH

group decreased to 1%wrt and then, beyond, it increased. Considering the evolution of the content of glyceryl monoacetate as seen in Fig.6(b), it confirmed that the tribocatalytic esterification of the solid superacid decreased the content of acetic acid and reduced acid corrosion of frictional surface.

In the O1s spectra, the peaks at 529.8eV and 531.5eV were ascribed to metal oxides (Fe_2O_3) and hydroxides (C-OH) [29]. The relative content of metal oxides was evaluated by the integral area ratio of I_a (Fe_2O_3) and I_b (C-OH). As the content of the solid superacid increased, the relative content of metal oxides increased at first and then decreased, the opposite of the carboxyl group (COOH). Similarly, the content of iron was the highest when lubricated with 1wt% the solid superacid as seen in Table 3. These behaviours are the likely result of tribocatalysis driving esterification, decreasing acid contents on the frictional surfaces and reducing corrosion.

The peaks at 710.9eV and 724.5eV in the Fe2p spectra belonged to Fe_2O_3, corresponding with the peak in the O1s spectra [30]. The peak at 169eV in the S2p spectra was ascribed to sulfates [31], most likely derived from the solid superacid. Hence, the frictional process resulted in a complex tribo-film comprising organics, metal oxides and sulfates.

Table 3 shows the chemical compositions of typical elements on the worn surfaces. It can be seen that there was no aluminium detected. This may be because elemental aluminium was too low relative to others. However, the elemental sulfur detected was indicative that sulfate ions may have been transfered from the solid superacid to the worn surfaces during frictional process, and in doing so will have

been deactivated [32].

A schematic diagram summarizing the effects of the solid superacid on tribological properties of the bio-oil is shown in **Fig.8**. When lubricated with pure bio-oil, severe abrasive wear resulted in a poor tribological response. This was most likely the results of acidic corrosion of frictional surface, and could be characterized by a high density of deep furrows and extreme exfoliation. The addition of solid superacid improved the tribologival properties of bio-oil. This was optimum at blend ratio of 1wt% solid superacid. This is likely to be a result of the particles rolling and polishing the frictional surface, which will have a positive effect on the tribological properties of bio-oil. Additionally, the solid superacid promoted tribocatalytic esterification and reduced acid driven corrosion of surfaces. At this ratio, the generated esters were absorbed on the friction surfaces improving the lubrication conditions. Beyond this level of solid superacid, at 2wt%, further absorption of esterified esters on to the may not have been possible. Furthermore, the increased particles may have led to larger agglomerations and severe abrasive wear, remove any benefical tribo-film and deactivating the solid superacid. In this case the acid corrosion of frictional surface will not have been reduced during rubbing. In combination, agglomeration and acid corrosion will have resulted in worse tribological properties.

4. Conclusions

In this work, novel in-situ tribocatalytic esterification reaction, based on varying

concentration of solid superacid (SO_4^{2-}/γ-Al_2O_3) has been developed as the catalyst and driven by frictional processes. The aims being to alleviate the corrosion wear induced by the high content of organic acid in bio-oil. Tests were conducted on an end-face friction and wear tester. Tribocatalytic esterification was evaluated by FTIR and GC-MS. The role of the solid superacid on the tribological durability of the friction surfaces was also examined. Several conclusions can be draw from this study and they are as follows:

1. The main wear mechanisms for pure bio-oil were abrasion and exfoliation driven by acidic corrosion.
2. The bio-oil with 1wt% solid superacid was the optimum ratio and possessed the best tribological properties. However, when the solid superacid (at all of the ratios studied) was added to the bio-oil, tribological properties improved. There was a two-fold effect behind the improvement
3. Mechanically, the solid superacid particles rolled through the contact zone and subsequently polished the frictional surfaces.
4. Chemically, the solid superacid catalyzed a tribocatalytic esterification reaction between acetic acid and glycerol that was driven by the frictional process. That is not to say that esterification could happen spontaneously, in the absence of the catalyst under the complicated tribological system. However, the solid superacid catalyst adds a degree of control to the process by promoting tribocatalytic esterification and increasing the conversion of acetic acid, which reduced acidic corrosion.

In combination the mechano-chemical effect synergistically improved the tribological properties of bio-oil. There was a limit to this improvement however, when the solid superacid was excessive (greater than 1% wrt in this case), severe friction may have deactivated solid superacid deactivate, coupled with excessive agglomeration lead to reduced tribological properties.

Acknowledgements:

This project is supported by the National Natural Science Foundation of China (Grant No. 51405124). Part of the experimental equipment used in this research, within the Birmingham Centre for Cryogenic Energy Storage, was obtained with support from the Engineering and Physical Sciences Research Council, under the eight great technologies: energy storage theme (grant number EP/L017725/1).

References

[1] Q. Lu, X.L. Yang, X.F. Zhu, Analysis on chemical and physical properties of bio-oil pyrolyzed from rice husk, J. Anal. Appl. Pyrolysis, 82 (2008) 191-198.

[2] D. Mohan, C.U. Pittman, P.H. Steele, Pyrolysis of Wood/Biomass for Bio-oil: A Critical Review, Energ. Fuel, 20 (2006) 848-889.

[3] X.J. Guo, S.R. Wang, Q. Wang, Z.G. Guo, Z.Y. Luo, Properties of Bio-oil from Fast Pyrolysis of Rice Husk, Chinese J. Chem. Eng., 19 (2011) 116-121.

[4] L. Ciddor, J.A. Bennett, J.A. Hunns, K. Wilson, A.F. Lee, Catalytic upgrading of bio-oils by esterification, J. Chem. Technol. Biot., 90 (2015) 780-795.

[5] Y.F. Xu, X.J. Zheng, X.G. Hu, Y.G. Yin, T.M. Lei, Preparation of the electroless Ni-P and Ni-Cu-P coatings on engine cylinder and their tribological behaviors under bio-oil lubricated conditions, Surf. Coat. Tech., 258 (2014) 790-796.

[6] X. Hu, R. Gunawan, D. Mourant, M.D.M. Hasan, L.P. Wu, Y. Song, C. Lievens, C.Z. Li, Upgrading of bio-oil via acid-catalyzed reactions in alcohols — A mini review, Fuel Process. Technol., 155 (2017) 2-19.

[7] M. Song, Z. P. Zhong, J.J. Dai, Different solid acid catalysts influence on properties and chemical composition change of upgrading bio-oil, J. Anal. Appl. Pyrolysis, 89 (2010) 166-170.

[8] J.J. Wang, J.Chang, J.Fan, Upgrading of Bio-oil by Catalytic Esterification and Determination of Acid Number for Evaluating Esterification Degree, Energ. Fuel, 24 (2010) 3251-3255.

[9] Y.F. Xu, X.J.Zheng, Y.B.Peng, B. Li, X.G. Hu, Y.G. Yin, Upgrading the lubricity of bio-oil via homogeneous catalytic esterification under vacuum distillation conditions, Biomass Bioenerg., 80 (2015) 1-9.

[10] K. Hiratsuka, C. Kajdas, Tribochemistry, tribocatalysis, and the negative-ion-radical action mechanism, P. I. Mech. Eng. J-J Eng., 223 (2009) 827-848.

[11] T. Onodera, K. Kawasaki, T. Nakakawaji, Y. Higuchi, N. Ozawa, K. Kurihara, M. Kubo, Tribocatalytic Reaction of Polytetrafluoroethylene Sliding on an Aluminum Surface, J. Phys. Chem. C, 119 (2015) 15954-15962.

[12] K. Hiratsuka, T. Abe, C. Kajdas, Tribocatalytic oxidation of ethylene in the rubbing of palladium against aluminum oxide, Tribol. Int., 43 (2010) 1659-1664.

[13] S.A. Rane, Esterification of Glycerol with Acetic Acid over Highly Active and Stable Alumina-based Catalysts: A Reaction Kinetics Study, Chem. Biochem. Eng. Q., 30 (2016) 33-45.

[14] J.A. Dean, Lange's Handbook of Chemistry, 15th ed., McGraw-Hill, New York, 1999.

[15] D.Y. Xu, H. Ma, F. Cheng, Preparation and application of zirconium sulfate supported on SAPO-34 molecular sieve as solid acid catalyst for esterification, Mater. Res. Bull., 53 (2014) 15-20.

[16] T. Luo, X.W. Wei, X. Huang, L. Huang, F. Yang, Tribological properties of Al_2O_3 nanoparticles as lubricating oil additives, Ceram. Int., 40 (2014) 7143-7149.

[17] Y.F. Xu, X.G. Hu, K. Yuan, G.L. Zhu, W.Z. Wang, Friction and wear behaviors of catalytic methylesterified bio-oil, Tribol. Int., 71 (2014) 168-174.

[18] S.F. Ren, J.H. Meng, J.B. Wang, J.J. Lu, S.R. Yang, Tribocorrosion behavior of Ti_3SiC_2 in the dilute and concentrated sulfuric acid solutions, Wear, 269 (2010) 50-59.

[19] P. Murkute, J. Ramkumar, S. Choudhary, K. Mondal, Effect of alternate corrosion and wear on the overall degradation of a dual phase and a mild steel, Wear, 368-369 (2016) 368-378.

[20] M.I.H.C. Abdullah, M.F.B. Abdollah, H. Amiruddin, N. Tamaldin, N.R.M. Nuri, Optimization of Tribological Performance of hBN/Al_2O_3 Nanoparticles as Engine Oil Additives, Procedia Engineering, 68 (2013) 313-319.

[21] Y.Y. Wu, W.C. Tsui, T.C. Liu, Experimental analysis of tribological properties of lubricating oils with nanoparticle additives, Wear, 262 (2007) 819-825.

[22] L. Peña-Parás, J. Taha-Tijerina, L. Garza, D. Maldonado-Cortés, R. Michalczewski, C. Lapray, Effect of CuO and Al_2O_3 nanoparticle additives on the tribological behavior of fully formulated oils, Wear, 332-333 (2015) 1256-1261.

[23] D. Jiao, S.H. Zheng, Y.Z. Wang, R.F. Guan, B.Q. Cao, The tribology properties of alumina/silica composite nanoparticles as lubricant additives, Appl. Surf. Sci., 257 (2011) 5720-5725.

[24] Z. Wu, H. Li, D.W. Tu, Application of Fourier Transform Infrared (FT-IR) Spectroscopy Combined with Chemometrics for Analysis of Rapeseed Oil Adulterated with Refining and Purificating Waste Cooking Oil, Food Anal. Method., 8 (2015) 2581-2587.

[25] A.A. Kuzharov, B.S. Luk'yanov, A.S. Kuzharov, Tribochemical transformations of glycerol, J. Frict. Wear, 37 (2016) 337-345.

[26] M.A. Fazal, A.S.M.A. Haseeb, H.H. Masjuki, Investigation of friction and wear characteristics of palm biodiesel, Energ. Convers. Manage., 67 (2013) 251-256.

[27] P. Taheri, J. Wielant, T. Hauffman, J.R. Flores, F. Hannour, J.H.W. de Wit, J.M.C. Mol, H. Terryn, A comparison of the interfacial bonding properties of carboxylic acid functional groups on zinc and iron substrates, Electrochim. Acta, 56 (2011) 1904-1911.

[28] F.D. Meng, Y.L. Yu, Y.M. Zhang, W.J. Yu, J.M. Gao, Surface chemical composition analysis of heat-treated bamboo, Appl. Surf. Sci., 371 (2016) 383-390.

[29] Y.F. Xu, X.J. Zheng, X.G. Hu, K.D. Dearn, H.M. Xu, Effect of catalytic esterification on the friction and wear performance of bio-oil, Wear, 311 (2014) 93-100.

[30] J.A. Ramos Guivar, E.A. Sanches, F. Bruns, E. Sadrollahi, M.A. Morales, E.O. López, F.J. Litterst, Vacancy ordered γ-Fe_2O_3 nanoparticles functionalized with nanohydroxyapatite: XRD, FTIR, TEM, XPS and Mössbauer studies, Appl. Surf. Sci., 389 (2016) 721-734.

[31] Z.Y. Xu, Y. Xu, K.H. Hu, Y.F. Xu, X.G. Hu, Formation and tribological properties of hollow sphere-like nano-MoS_2 precipitated in TiO_2 particles, Tribol. Int., 81 (2015) 139-148.

[32] H. Song, L. Zhao, N. Wang, F. Li, Isomerization of n-pentane over La-Ni-$S_2O_8^{2-}$/ZrO_2-Al_2O_3 solid superacid catalysts: Deactivation and regeneration, Appl. Catal. A: Gen., 526 (2016) 37-44.

Table and Figure Captions

Table 1 Tribological testing conditions.

Table 2 Relative atomic percentage of elemental carbon in different valence states on the worn surfaces with different concentrations of the solid superacid.

Table 3 Chemical compositions of typical elements on worn surfaces with different concentrations of the solid superacid.

Fig. 1 Schematic diagram of the friction pairs and the tribometer.

Fig. 2 SEM micro-morphology and EDS spectrum of the solid superacid.

Fig. 3 (a) Particle size distribution of the solid superacid, (b) FTIR spectra of the solid superacid and γ-Al_2O_3 powders, and (c) conversion rate of acetic acids with time with 2 wt% the solid superacid at 120 °C.

Fig. 4 (a) Average friction coefficient, and (b) wear loss with different concentrations of the solid superacid.

Fig. 5 SEM micro-morphologies of worn surfaces with different concentrations of the solid superacid: (a) 0wt%, (b) 0.5wt%, (c) 1wt%, (d) 1.5wt% and (e) 2wt%.

Fig. 6 (a) FTIR spectra, (b) Gas Chromatograms of bio-oil with different concentrations of the solid superacid, and (c) the mass spectrum of glyceryl monoacetate.

Fig. 7 XPS spectra of typical elements on worn surfaces with different concentrations of the solid superacid.

Fig. 8 Schematic diagram of the effect of the solid superacid during the frictional process.

Table 1 Tribological testing conditions.

Testing conditions	Values
Normal load / N	600
Contact pressure / MPa	12.5
Rotational speed / rpm	441
Rotating diameter / mm	26
Temperature / °C	25
Duration / min	60

Table 2 Relative Relative atomic percentage of elemental carbon in different valence states on the worn surfaces with different concentrations of the solid superacid.

The solid superacid content (wt%)	Relative atomic percentage of carbon (at %)			
	284.7 C-C/C-H	285.7 C-O	288.3 COOC	289.1 COOH
0	64.38	24.03	6.57	5.02
0.5	69.87	19.76	6.57	3.80
1	78.09	13.86	6.63	1.42
1.5	67.59	24.05	4.55	3.81
2	64.51	26.73	4.73	4.03

Table 3 Chemical compositions of typical elements on worn surfaces with different concentrations of the solid superacid.

Solid superacid concentration (wt%)	Chemical composition (at %)				
	C	O	Fe	S	Al
0	60.16	31.89	7.95	/	/
0.5	55	35.14	8.8	1.06	/
1	53.3	35.85	10.85	/	/
1.5	56.37	31.71	8.21	3.71	/
2	55.78	33.35	8.81	2.06	/

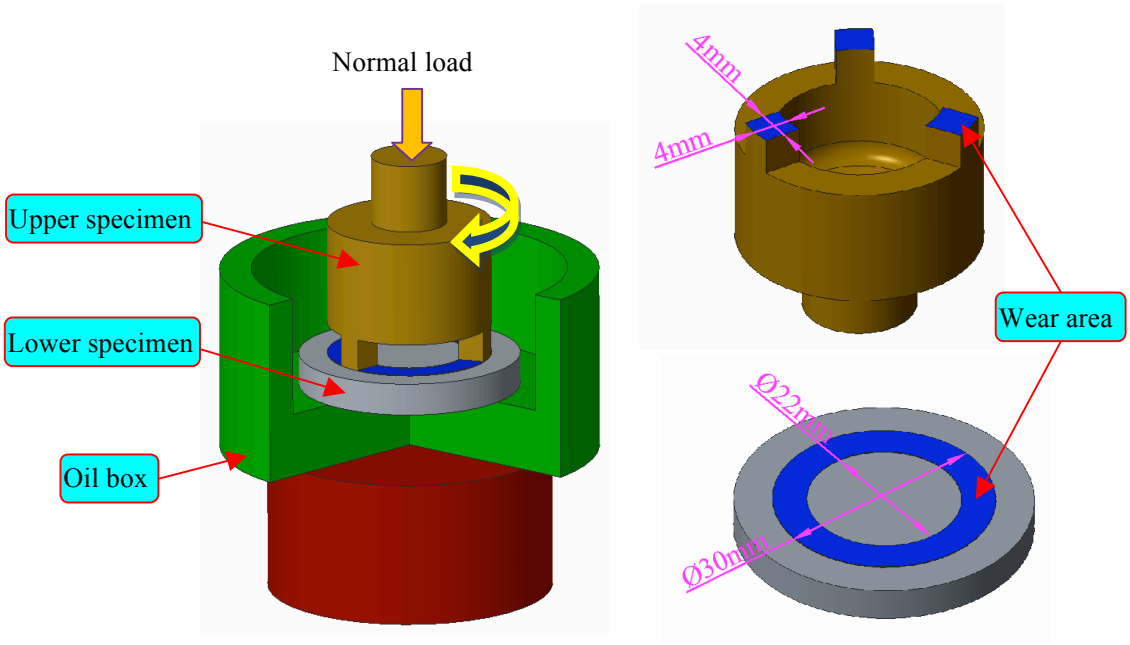

Fig. 1 Schematic diagram of the friction pairs and the tribometer.

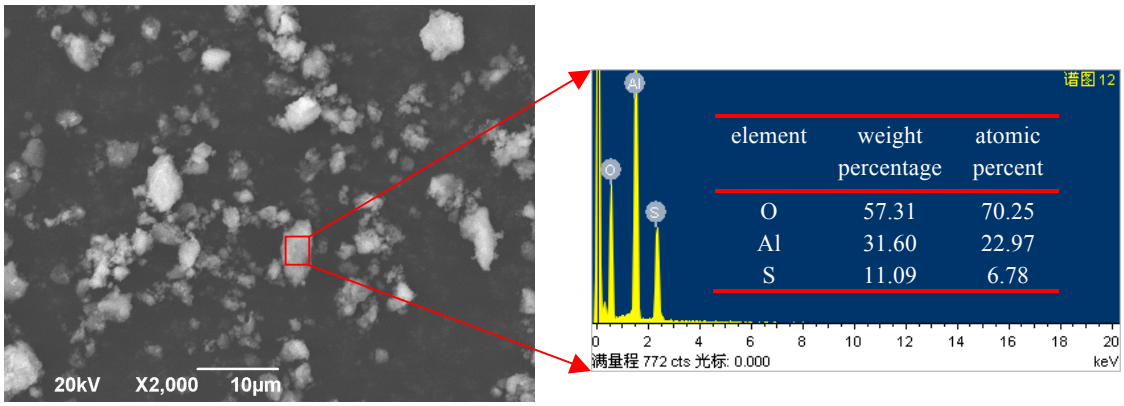

Fig. 2 SEM micro-morphology and EDS spectrum of the solid superacid.

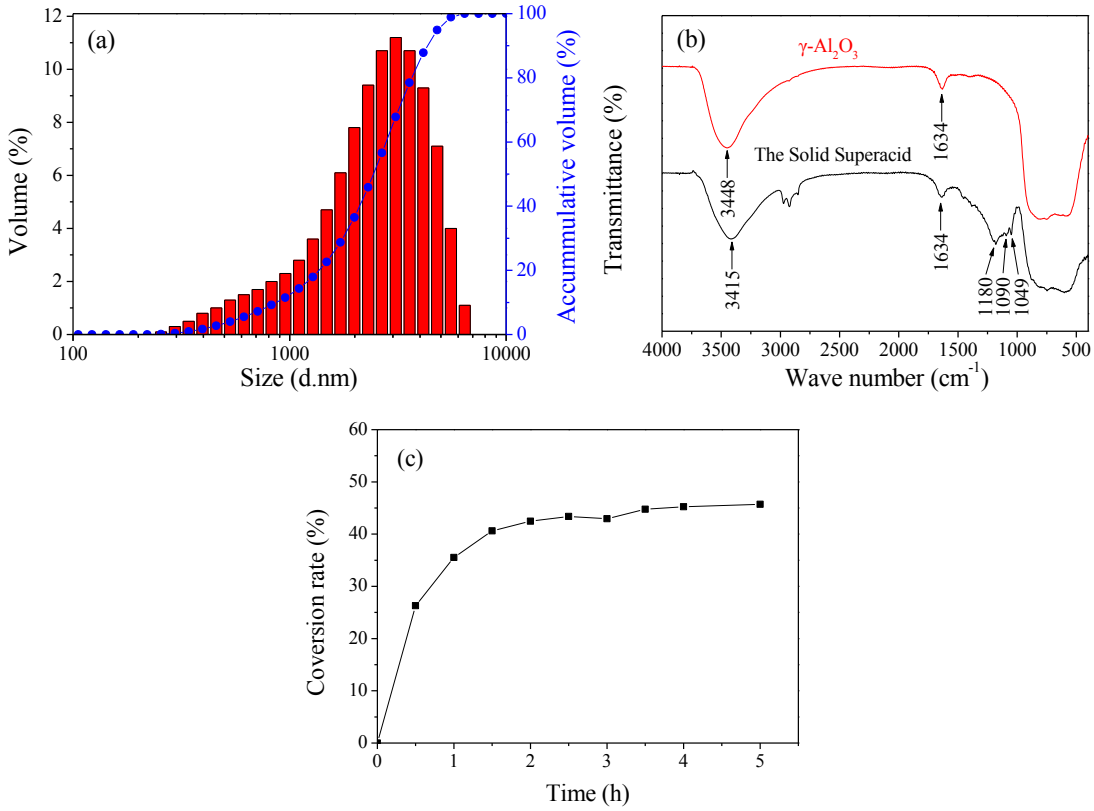

Fig. 3 (a) Particle size distribution of the solid superacid, (b) FTIR spectra of the solid superacid and γ-Al_2O_3 powders, and (c) conversion rate of acetic acids with time with 2 wt% the solid superacid at 120 °C.

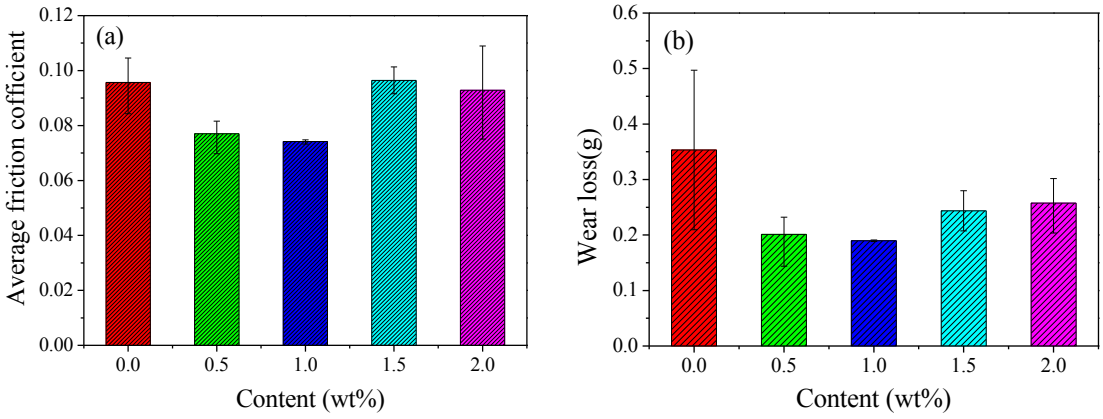

Fig. 4 (a) Average friction coefficient, and (b) wear loss with different concentrations of the solid superacid.

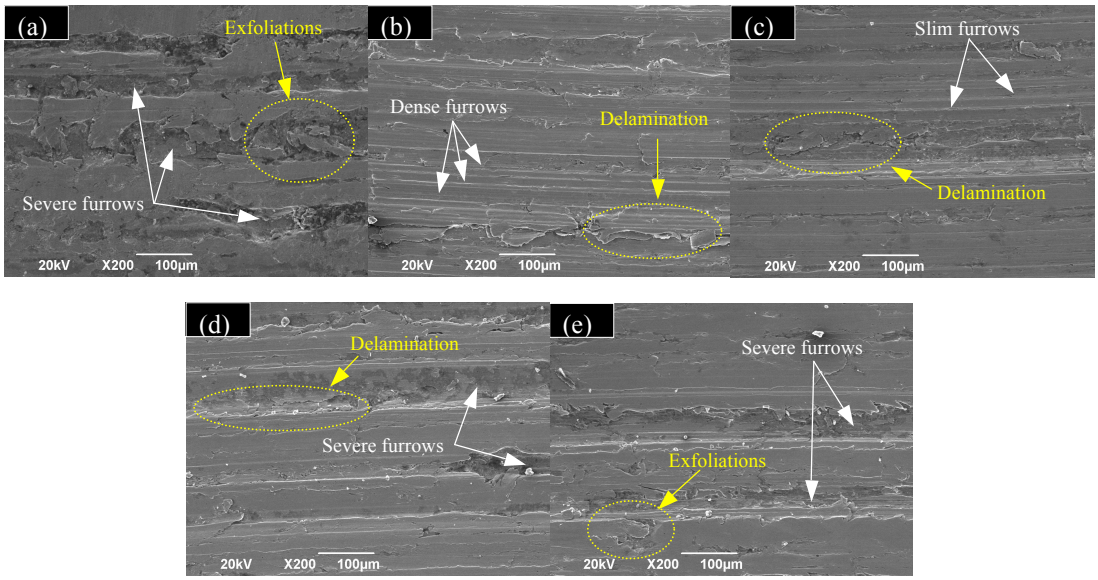

Fig. 5 SEM micro-morphologies of worn surfaces with different concentrations of the solid superacid: (a) 0wt%, (b) 0.5wt%, (c) 1wt%, (d) 1.5wt% and (e) 2wt%.

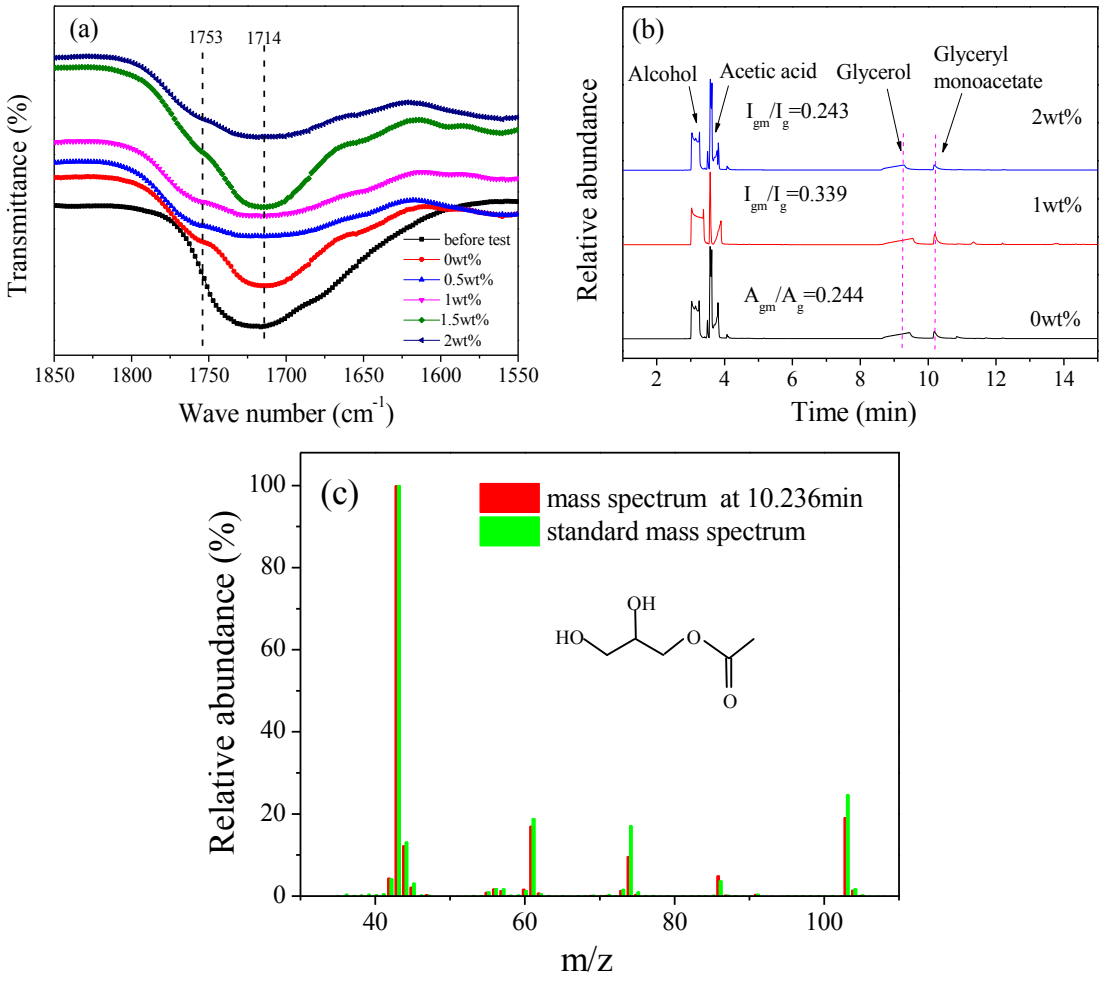

Fig. 6 (a) FTIR spectra, (b) Gas Chromatograms of bio-oil with different concentrations of the solid superacid, and (c) the mass spectrum of glyceryl monoacetate.

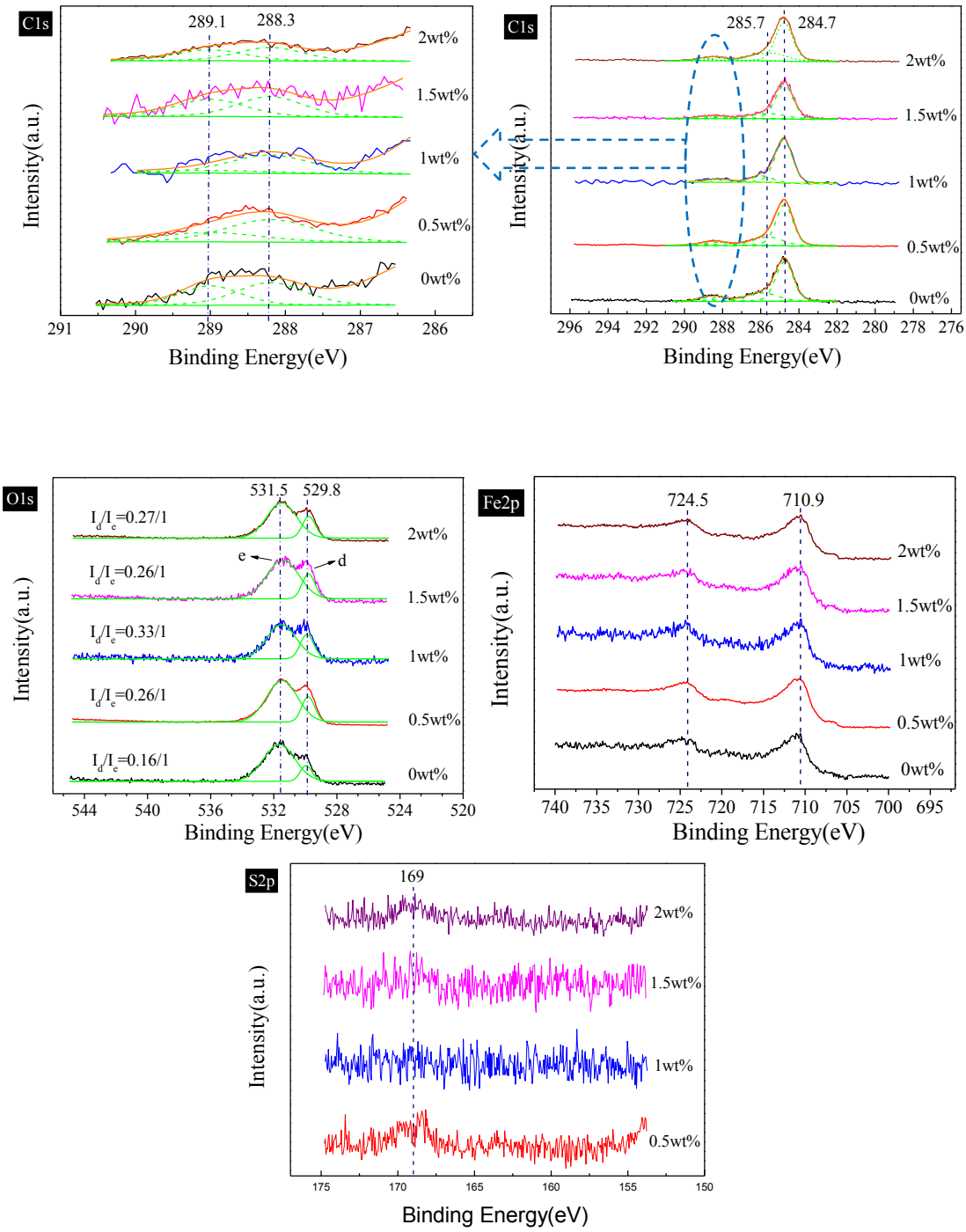

Fig. 7 XPS spectra of typical elements on worn surfaces with different concentrations of the solid superacid.

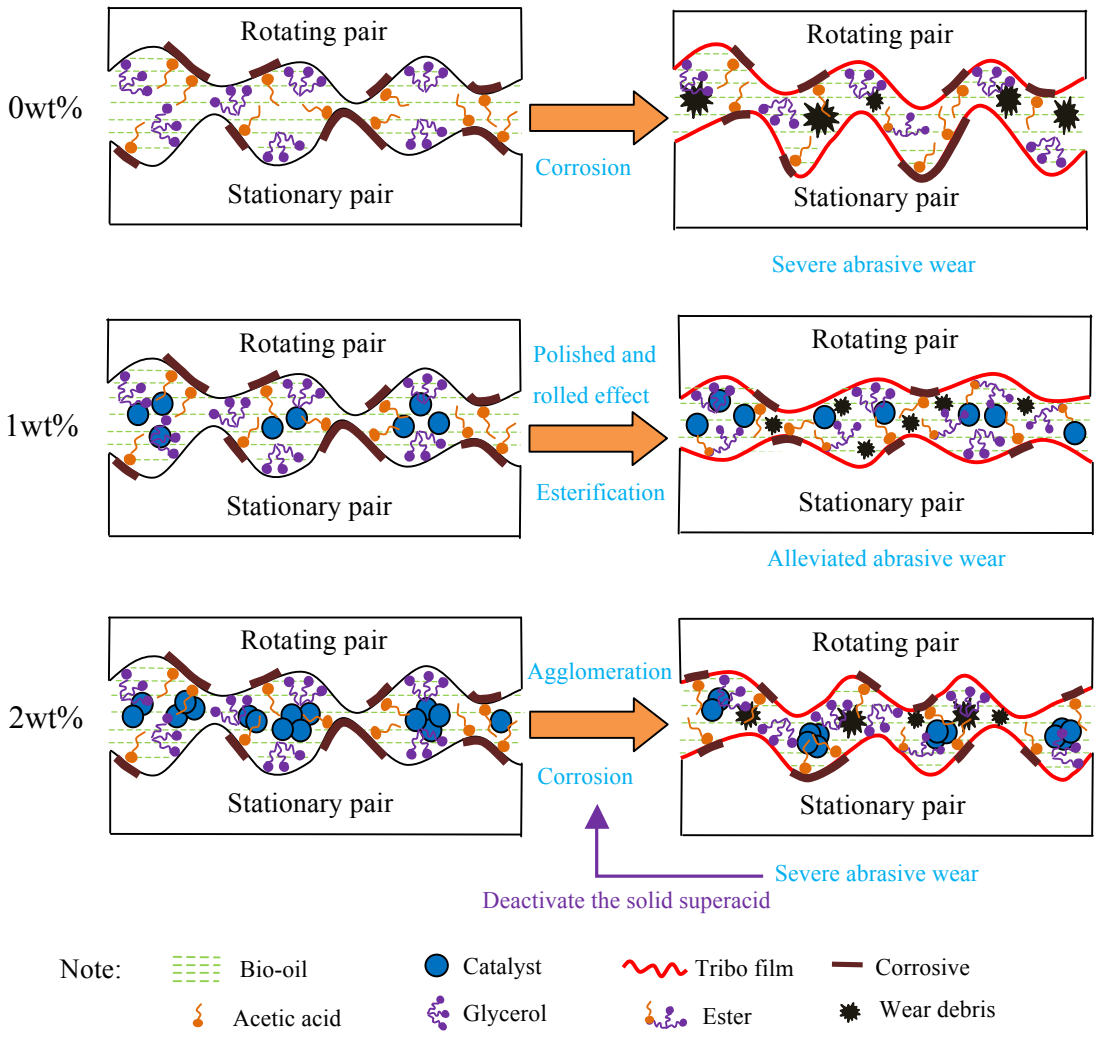

Fig. 8 Schematic diagram of the effect of the solid superacid during the frictional process.